ELSEVIER

Biochimica et Biophysica Acta 1513 (2001) 167–175

BIOCHIMICA ET BIOPHYSICA ACTA
BBA

www.bba-direct.com

Self-assembly of influenza hemagglutinin: studies of ectodomain aggregation by in situ atomic force microscopy

Raquel F. Epand [a], Christopher M. Yip [b], Leonid V. Chernomordik [c], Danika L. LeDuc [d], Yeon-Kyun Shin [e], Richard M. Epand [a,*]

[a] *Department of Biochemistry, McMaster University, Hamilton, ON, Canada, L8N 3Z5*
[b] *Department of Chemical Engineering and Applied Chemistry, Institute of Biomaterials, and Biomedical Engineering, University of Toronto, Toronto, ON, Canada, M5S 3G9*
[c] *Section on Membrane Biology, LCMB, NICHD, NIH, Bethesda, MD 20892-1855, USA*
[d] *Department of Chemistry, University of California, Berkeley, CA 94720, USA*
[e] *Department of Biochemistry and Biophysics, Iowa State University, Ames, IA 50011, USA*

Received 14 March 2001; received in revised form 1 May 2001; accepted 3 May 2001

Abstract

We have used in situ tapping mode atomic force microscopy (AFM) to study the structural morphology of two fragments of the influenza hemagglutinin protein bound to supported bilayers. The two proteins that we studied are the bromelain-cleaved hemagglutinin (BHA), corresponding to the full ectodomain of the hemagglutinin protein, and FHA2, the 127 amino acid N-terminal fragment of the HA2 subunit of the hemagglutinin protein. While BHA is water soluble at neutral pH and is known to bind to membranes via specific interactions with a viral receptor, FHA2 can only be solubilized in water with an appropriate detergent. Furthermore, FHA2 is known to readily bind to membranes at neutral pH in the absence of a receptor. Our in situ AFM studies demonstrated that, when bound to supported bilayers at neutral pH, both these proteins are self-assembled as single trimeric molecules. In situ acidification resulted in further lateral association of the FHA2 without a large perturbation of the bilayer. In contrast, BHA remained largely unaffected by acidification, except in areas of exposed mica where it is aggregated. Remarkably, these results are consistent with previous observations that FHA2 promotes membrane fusion while BHA only induces liposome leakage at low pH. The results presented here are the first example of in situ imaging of the ectodomain of a viral envelope protein allowing characterization of the real-time self-assembly of a membrane fusion protein.

Keywords: Atomic force microscopy; Membrane fusion; Bromelain-cleaved hemagglutinin; Protein–lipid interactions

1. Introduction

Influenza virus hemagglutinin (HA) is a trimeric protein with each monomer being comprised of two disulfide-linked polypeptide chains, HA1 and HA2. The low pH form of HA promotes the fusion of the viral envelope with an endosome membrane during viral entry. The HA1 chain contains the receptor

Abbreviations: AFM, atomic force microscopy; TMAFM, tapping mode AFM; HA, influenza hemagglutinin; BHA, bromelain-cleaved HA; FHA2, residues 1–127 of the HA2 polypeptide chain of the influenza hemagglutinin; DOPC, dioleoylphosphatidylcholine; DOPE, dioleoylphosphatidylethanolamine

* Corresponding author. Fax: 905-521-1397.
E-mail address: epand@mcmaster.ca (Richard M. Epand).

0005-2736/01/$ – see front matter
PII: S0005-2736(01)00350-9

binding domain, while the HA2 chain contains the fusion peptide that inserts into the target membrane [1]. The protein is attached to the membrane via a single transmembrane helical segment in the HA2 subunit. HA was the first membrane fusion protein to be successfully crystallized [2]. While single crystals of the entire ectodomain of HA (BHA) could be isolated at neutral pH, the low pH form of BHA must be truncated in order to facilitate crystallization [3]. Under acidic conditions but in the absence of membranes, BHA is known to undergo a large conformational rearrangement resulting in a coiled-coil structure that closely resembles that of other active membrane fusion proteins [4].

Most of the information about the structure of HA in a membrane environment comes from electron microscopy. Previous negative stain transmission electron microscopy and antibody binding studies have suggested that the influenza HA protein inserts its fusion peptide into the viral membrane [5]. Using cryo-electron microscopy, Shangguan and coworkers showed that the kinetics of the acid-induced conformational change in HA was too slow to account for the pH dependence of fusion [6]. Cryo-electron microscopy has also been used to postulate a model for the structure of the intact HA trimer [7].

BHA is a water-soluble protein that does not spontaneously partition into a membrane lacking a receptor at neutral pH. Under acidic conditions BHA will spontaneously form rosettes in solution [8]. The protein will bind specifically to sialic acid-containing membranes at neutral pH, owing to a binding site on the HA1 subunit. At low pH BHA is known to induce liposome leakage but not significant membrane fusion, and it rapidly becomes inactivated [9]. The structure of the membrane-associated protein and/or the actual extent of aggregation or oligomerization at the membrane surface remain unknown [8].

FHA2 is the major portion of the HA2 subunit of BHA. It comprises the first 127 amino acids of the ectodomain and has no receptor binding function. Unlike BHA, in which the hydrophobic fusion peptide is sequestered within the protein structure at neutral pH, the fusion peptide of FHA2 is exposed at the end of the coiled-coil region and FHA2 can bind to membranes lacking a receptor at neutral pH [10]. As with the holoprotein, FHA2 will form trimers in solution [10]; however, similar to BHA, the state of oligomerization of this construct on membranes and its extent of oligomerization as a function of pH are not known. Although FHA2 promotes membrane fusion when measured with a lipid mixing assay, this fusion is also leaky [11]. It remains unclear as to why FHA2, which comprises only a segment of the HA2 subunit, is more active in promoting lipid mixing than BHA, which contains a larger segment of HA2 as well as the HA1 subunit and is more similar structurally to the HA of native intact virus.

It has now been shown that FHA2 can induce hemifusion of cells with a potency comparable to that of the intact hemagglutinin [12]. The structure of the membrane-bound HA or any of its fragments is not known. At acidic pH, where the protein is fusion-active, the only known HA-related crystal structure is that of a truncated form of HA2 that lacked the segments essential for fusogenic activity. In situ atomic force microscopy (AFM) has been used previously to study protein–lipid interactions [13–17]. In the present work we have studied the association of two different forms of the ectodomain of the influenza HA at supported lipid bilayer interfaces as a function of pH and incubation time. These studies are the first example of the application of atomic force microscopy to a study of the properties of the hemagglutinin protein of influenza virus. The results provide direct evidence of different protein aggregation phenomena at model lipid surfaces for the BHA and FHA2 fragments of the influenza HA, that may be relevant to their function.

2. Materials and methods

2.1. Materials

FHA2 from the X-31 strain of the influenza virus was expressed in *Escherichia coli* BL21(DE3) as previously described [18]. The final preparation of FHA2 was 100 μM peptide in 0.1% Triton X-100, 500 mM NaCl, 0.4 mM DTT, 1 mM EDTA, 1 mM PMSF, 5 mM citrate–phosphate buffer, pH 7.0. BHA, from the PR/8/34 strain of influenza virus, was prepared by Spafas (Storrs, CT, USA) according

to the procedure of Compans et al. [19]. Another preparation of BHA, made by bromelain cleavage of influenza A X-31, was kindly provided to us by Drs. J.M. White and J.A. Gruenke.

All phospholipids used in this work were purchased from Avanti Polar Lipids (Alabaster, AL, USA). The ganglioside, G_{D1a}, was purchased from Dr. I. Mikhalyov (Moscow, Russia).

2.2. Preparation of samples for AFM

Lipids in the desired ratio were combined in a solution of chloroform/methanol (2:1; v/v). For FHA2 studies, bilayers composed of equimolar amounts of dioleoylphosphatidylcholine (DOPC), dioleoylphosphatidylethanolamine (DOPE) and cholesterol were prepared; for BHA studies, the same lipid composition was used but containing an additional 5% of ganglioside G_{D1a}. The lipids were deposited on the wall of a glass test tube by solvent evaporation under a stream of nitrogen. Last traces of solvent were removed under vacuum for 2 h. The film was hydrated with 5 mM HEPES, 5 mM MES, 5 mM citric acid, 0.15 M NaCl and 1 mM EDTA, pH 7.4 (HEPES–MES–citrate) to give a final lipid suspension of 1 mg/ml. This suspension was then placed in a bath type sonicator for approx. 20 min, until the suspension became clear or only slightly hazy. This lipid suspension was then applied to the surface of freshly cleaved mica and the lipid allowed to adhere to the mica surface over a period of 10–20 min.

2.3. Atomic force microscopy

Solution tapping mode atomic force microscopy (TMAFM) images were acquired on a Digital Instruments Nanoscope IIIA MultiMode scanning probe microscope (Digital Instruments, Santa Barbara, CA, USA) using 120 μm oxide-sharpened silicon nitride V-shaped cantilevers installed in a combination contact/tapping mode liquid flow cell. The flow cell was fitted with inlet and outlet tubes to enable direct fluid exchange during imaging. The AFM cantilevers were irradiated with UV light prior to imaging to remove any adventitious organic contaminants. The AFM images were acquired using the E scanning head, which has a maximum lateral scan area of 14.6 μm×14.6 μm. All imaging was performed at tip scan rates from 1.25 to 2 Hz, using cantilever drive frequencies of approx. 8.9 kHz at ambient temperature. All images were captured as 512×512 pixel images and were low-pass filtered. Feature size and volumes were calculated using the Digital Instruments Nanoscope software (version 4.21) and shareware image analysis program, NIH-Image (version 1.62). Supported bilayers were formed by directly injecting approx. 500 μl of the 1 mg/ml lipid suspension into the AFM fluid cell, previously sealed against a piece of freshly cleaved mica and allowing the vesicles to fuse in situ. The cell was flushed with buffer and reference TMAFM height and phase images acquired in protein-free HEPES–MES–citrate buffer at pH 7.4 to confirm formation of stable lipid bilayers. Approx. 500 μl of the protein solution in HEPES–MES–citrate buffer was added and the sample imaged again to obtain reference images of the membrane-associated proteins. The solution of FHA2 was diluted 100-fold from the stock and contained only 0.001% Triton X-100. This concentration of detergent is not sufficient to prevent insertion of the protein into membranes or to inhibit fusion [11]. Since the AFM fluid cell volume is approx. 200 μl, we have ensured complete replacement of the original imaging buffer prior to introducing the protein or exchanging the buffer. The imaging buffer was then exchanged by the direct addition of approx. 500 μl of a protein-free HEPES–MES–citrate buffer at pH 5.0 and the imaging reinitiated. At no time was the AFM cell removed from the mica surface nor was the lipid bilayer exposed to air.

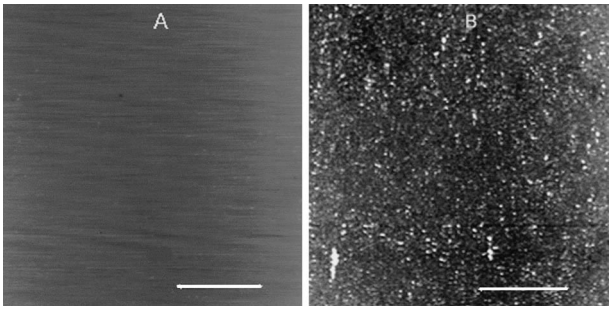

Fig. 1. In situ tapping mode AFM images. (A) A bilayer composed of DOPC:DOPE:cholesterol (1:1:1) at pH 7.4. (B) After introduction of a concentrated solution of FHA2 (100 μg/ml) at pH 7.4, showing coverage of the bilayer surface with particles of protein. Image sizes: 10 μm×10 μm. Calibration bar: 2.86 μm.

3. Results

The in situ fusion of sonicated lipid vesicles comprising an equimolar mixture of DOPC, DOPE and cholesterol ($\pm 5\%$ G_{D1a}) to a mica surface resulted in the formation of approx. 5 nm thick, planar bilayers, substantially defect-free and flat on a molecular scale (Fig. 1A). This surface, imaged initially in the presence of buffer at pH 7.4, was free of debris. The direct addition of FHA2 to the AFM liquid cell resulted in the deposition of ellipsoidal FHA2 molecules on the bilayer. Using a solution of 100 μg/ml FHA2 at pH 7.4, many small particles were observed on the bilayer surface (Fig. 1B). Using a more dilute solution of FHA2 (10 μg/ml) resulted in the sporadic deposition of particles on the bilayer surface. This allowed for a more accurate estimation of size of an individual particle, which averaged approx. 7×14 nm with an overall thickness (or height) above the bilayer surface of approx. 2 ± 0.6 nm. The length is consistent with that observed by Wharton et al. [5] using electron microscopy. Although AFM tip effects contribute to an overestimation of lateral feature dimensions, the measured vertical distances are largely unaffected by the imaging forces, provided appropriate measures are taken to account for surface charge and double-layer forces [20,21]. Previous work has demonstrated that one can readily balance the forces between the AFM tip and the surface of interest by appropriate selection of the imaging fluid and thus adjustment of the Hamaker constant [22]. Although there is some heterogeneity, a large fraction of smaller particles have dimensions consistent with FHA2 binding to the membrane surface as a single trimer. We did not observe growth of the surface aggregates with time under these neutral pH conditions. However, after several minutes at pH 7.4 the height of the particles measured decreased to approx. 1 nm above the bilayer surface, suggesting a tendency of the protein to sink into the bilayer with time.

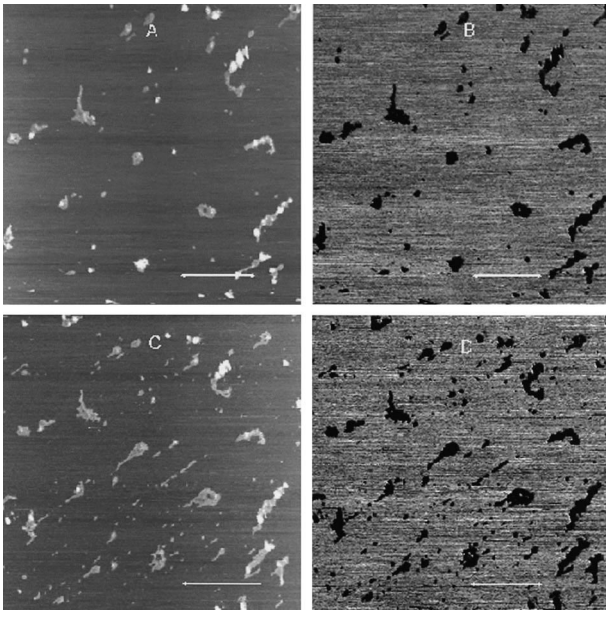

Fig. 2. In situ tapping mode AFM images of the FHA2 aggregates on a DOPC:DOPE:cholesterol (1:1:1) bilayer formed over mica. FHA2 was bound to the bilayer after being introduced as a 10 μg/ml solution at pH 7.4, and was then acidified to pH 5.0. (A) 52 min after acidification, in height mode; (B) 52 min after acidification, in phase mode; (C) 79 min after acidification, in height mode; (D) 79 min after acidification, in phase mode. Image sizes: 5 μm × 5 μm. Calibration bar: 1.20 μm.

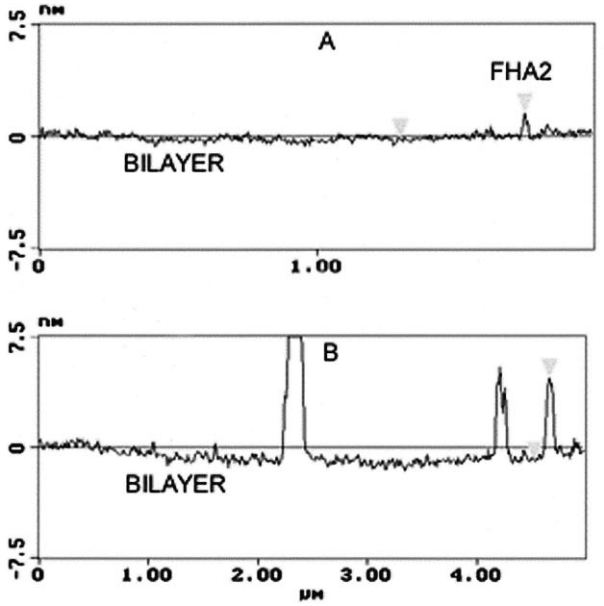

Fig. 3. Image section analysis. (A) Height of a particle of FHA2, deposited from a 10 μg/ml solution of FHA2 at pH 7.4, with respect to the bilayer; particle height is 2 nm. (B) Aggregates of FHA2 formed 52 min after acidification to pH 5 of the same solution deposited in A; particle heights are 17 nm (off scale on the figure), 6.5 nm and 5 nm.

Remarkably, upon in situ acidification, we observed the direct association of the individual FHA2 particles across the bilayer surface (Fig. 2A–D). This association process at acidic pH progressed over time. This recruitment of particles occurs de-

spite the fact that the solution in contact with the membrane was displaced by acidic buffer. Because of the change in dimensionality between the two-dimensional lipid surface and the three-dimensional volume of solution above it, it would not require much residual protein in the supernatant to result in further deposition to the membrane. Extensive washing of the specimen could result in removal of some of the protein that adhered at neutral pH. The height of some of particles is shown for a 10 μg/ml solution of FHA2 at pH 7.4 (Fig. 3A) and at pH 5.0 (Fig. 3B). There is a marked change in both height and heterogeneity of the particles at acidic pH, where some of the larger aggregates reach a value of approx. 20 nm.

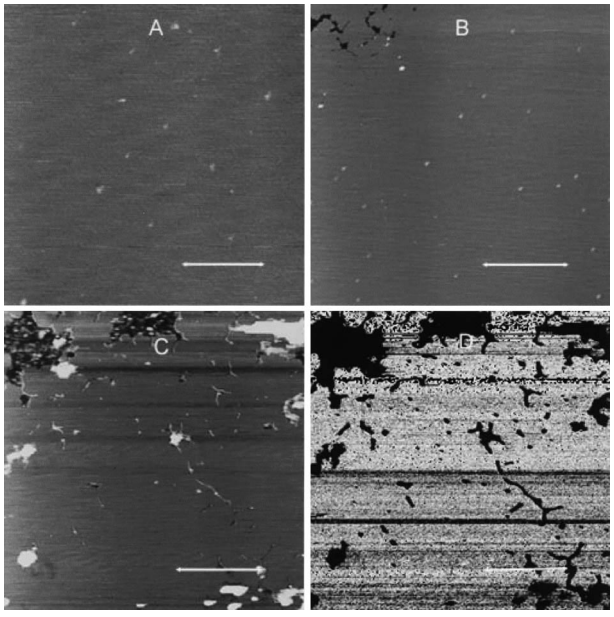

Fig. 4. In situ tapping mode AFM images of the BHA prepared from PR/8 aggregates bound to the surface of a DOPC:DOPE:cholesterol (1:1:1) bilayer containing 5% G_{D1a}. (A) At pH 7.4 after adding to a bilayer deposited on mica. (B) 28 min after acidification to pH 5. The darker regions in the upper left-hand corner are defects in the approx. 5 nm thick lipid bilayer that expose the underlying mica substrate. (C) 116 min after acidification. Note that the area of exposed mica is larger in this image. Within this area one can observe protein particles. There are protein aggregates associated with either line defects or larger regions of exposed mica. In addition, many BHA particles whose size has not changed as a result of acidification are also present. (D) The identical image as in C but in phase mode, rather than height mode, to clearly demonstrate the line defects. Image sizes: (B,C,D) 5 μm×5 μm; calibration bar: 1.34 μm; (A) 2 μm×2 μm; calibration bar: 0.52 μm.

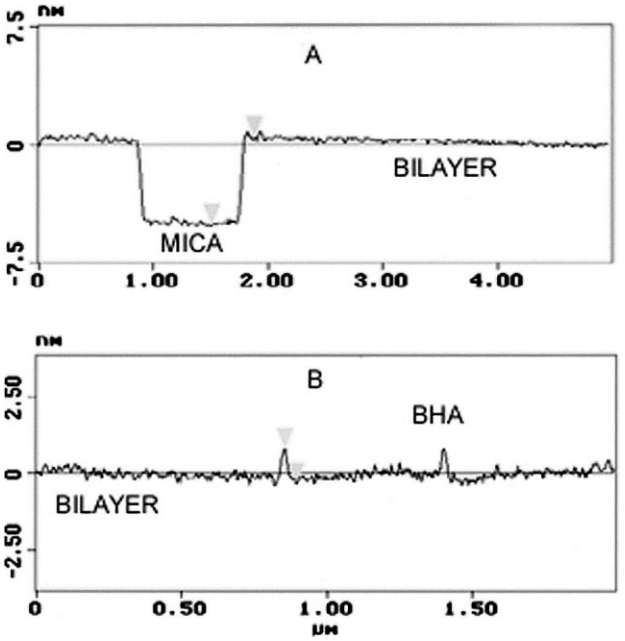

Fig. 5. Image section analysis of a bilayer composed of a DOPC:DOPE:cholesterol (1:1:1) containing 5% G_{D1a}. (A) A break in the bilayer showing a 5 nm depth between the mica and the bilayer surface. (B) Deposited BHA particles rising to 2 nm above the bilayer, at pH 7.4.

To complement our study of the FHA2 fragment, two preparations of BHA were studied under similar conditions. While BHA prepared from the X-31 influenza strain did not bind to the membrane at pH 7.4, in situ acidification with pH 5.0 protein-free buffer led to the deposition of small BHA aggregates on the membrane. The lack of BHA binding at pH 7.4 from this particular influenza strain can be explained by the greater specificity of this strain for specific sialolipids, particularly certain neolactogangliosides [23]. However, the PR/8 strain of influenza exhibits a lower specificity for binding to sialylated moieties [23] and is known to bind to G_{D1a} [24,25]. We find that when BHA is prepared from the PR/8 strain, binding does occur at neutral pH to membranes containing G_{D1a} (Fig. 4A). A typical BHA particle appears as an oblate ellipsoid with an average diameter of approx. 17.5 nm in the plane of the membrane and extending approx. 2 nm above the plane of the membrane (Fig. 5B). The smooth, 5 nm thick bilayer is shown for comparison (Fig. 5A). The observed diameter of the BHA is consistent with a diameter of 15 nm determined by electron microsco-

py [5] and it is of the order of magnitude expected for a single BHA trimer.

In direct contrast to the results seen for the FHA2 fragment, exchange of the pH 7.4 imaging buffer with a protein-free pH 5.0 buffer with the same chemical composition did not drastically alter the state of BHA oligomerization (Fig. 4B). The lack of extensive aggregation of BHA at acidic pH is not a consequence of the presence of G_{D1a} in the membrane, since we observe that this ganglioside does not prevent the aggregation of FHA2 in the membrane. At acidic pH, the two forms of BHA made from different strains of influenza appear similar, as does the underlying bilayer.

Upon acidification to pH 5 in the presence of BHA, we observe the appearance of small bilayer defects and holes (see upper left-hand corner of Fig. 4B). With increased time these defects grow and large aggregates of BHA form only in regions close to these defects (Fig. 4C,D). The in situ acidification of the bilayer in the absence of BHA did not result in bilayer disruption. There was no Triton used in the experiment with BHA, thus the observed holes were not caused by damage due to detergent. In addition, BHA at acidic pH also induces line defects (Fig. 4C) that are also associated with aggregated particles. The presence of these line defects is clearly visible in the phase mode (Fig. 4D); they protrude approx. 1 nm above the bilayer. There are also a few large aggregates that may have moved away from the defect regions. These defects are not likely to be caused by the extended duration of imaging since we find in all our experiments that this did not damage the lipid bilayer or the adsorbed aggregates. We cannot, however, entirely rule out that the sweeping action of the imaging tip serves to increase convective flow of soluble protein into the imaging frame. However, low-resolution, large area scans did not reveal any evidence of tip-induced aggregation. It appears more likely then that the protein itself induces these defects, although the mechanism by which this occurs is not known.

4. Discussion

There are marked differences in the aggregation behavior of FHA2 and BHA as a function of pH. While both constructs form trimers on the membrane surface at neutral pH, the FHA2 underwent extensive further lateral association on the bilayer upon acidification of the medium. There is evidence to indicate that in the absence of HA1, a single FHA2 trimer is in an extended coiled-coil conformation at

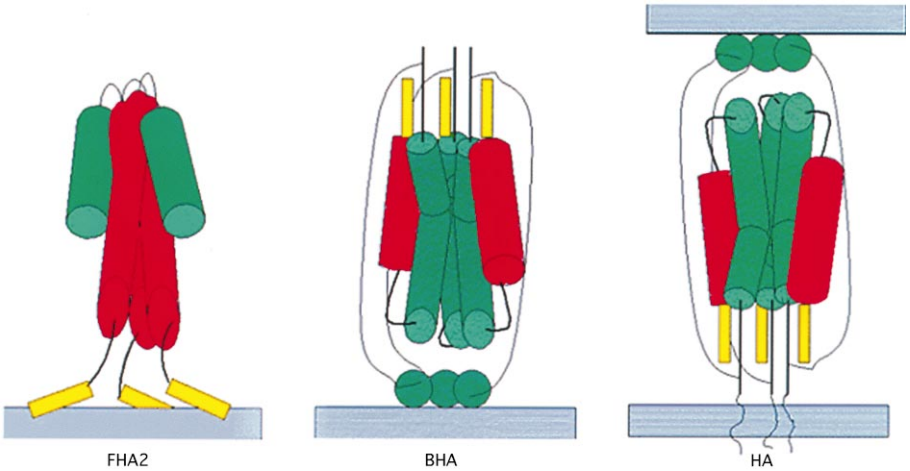

Fig. 6. Schematic diagram showing the relationship between the various proteins used in this work and the membrane at pH 7. Both BHA and HA must initially be in a vertical orientation with respect to the plane of the membrane in order to bridge two membranes to initiate fusion. Membrane, blue; fusion peptide, yellow; helical segments are colored green or red for visual contrast; other polypeptide segments, black lines; globular domain of HA1, in green. Only in the case of HA are there two membranes, the viral membrane and the target membrane. HA is oriented with its fusion peptide facing in the same direction as for FHA2. Note that this orientation is not possible for BHA because it is attached to the membrane from the opposite end of the protein.

both neutral and acidic pH. The fusion peptide of FHA2 is an exposed hydrophobic segment that can spontaneously enter the membrane at neutral pH as indicated by spin labeling studies [10,18]. In contrast to FHA2, the BHA protein is water-soluble and at neutral pH will bind only to exposed sialic acid residues at the membrane interface. Examination of the crystal structure of BHA reveals that at neutral pH, BHA will adopt a folded compact conformation [2].

Despite lack of evidence for a conformational change in FHA2 upon acidification, this protein undergoes extensive pH-dependent aggregation (Fig. 2). This aggregation continues well beyond the time required for liposome fusion [11]. It is thus likely that this aggregation process is at least in part associated with the process of inactivation that is known to occur with FHA2 at acidic pH [11]. The pH-dependent aggregation is likely to be associated with the exposure of new hydrophobic groups on this peptide, as has been demonstrated by ANS binding [26]. These groups are in regions other than the fusion peptide that is already exposed at neutral pH.

The aggregation properties of BHA are quite different. There is little if any increase in size of BHA upon acidification in regions in which the bilayer is intact. ANS binding experiments indicate that acidification of BHA also leads to an increase in the extent of exposure of hydrophobic groups [27]. However, the kinetics of increased ANS binding after acidification is much slower for BHA than for FHA2 [26] or for the intact HA [28]. In the case of FHA2, the increased ANS binding with acidification is not simply a consequence of the reduction of charge repulsion since some constructs with single amino acid replacements do not show this effect [26]. This slower exposure of hydrophobic groups may be the cause for the different effects on the membrane. Upon acidification, BHA appeared to initiate defects in the previously intact bilayer (Fig. 4B–D). This action would be consistent with the observation that BHA induces vesicle leakage at acidic pH [9]. BHA, however, did form some aggregates that appeared to be associated either with line defects or with regions of exposed mica at low pH. Aggregates are not observed prior to defect formation and the first aggregates are seen within a region of exposed mica. However, at longer times some aggregates are observed outside of the region of exposed mica, likely as a consequence of diffusion subsequent to their formation on the exposed mica surface. Remarkably, BHA does not promote rapid lipid mixing with liposomes of the same composition (unpublished observations).

Our results suggest that a protein's ability to expose hydrophobic residues and aggregate at acidic pH is closely associated with its ability to enhance membrane fusogenicity. Thus, FHA2 that aggregates at low pH is also fusogenic at low pH, while BHA, which is not fusogenic, appears not to aggregate on the surface of the bilayer. Aggregation of the intact HA protein has also been shown to be required for fusion [29–32]. This initial aggregation to form small clusters of HA is required for the formation of the fusion intermediate, while more extensive aggregation at longer times is associated with inactivation [33]. The difference in aggregation behavior on the surface of a membrane among FHA2, BHA and intact HA can be understood in terms of the morphological relationship between the domain with which the protein binds to a membrane and the location of the fusion peptide relative to the membrane. The spatial relationship of these constructs when bound to a membrane at pH 7 is depicted in Fig. 6. The fusion peptide is very hydrophobic and likely to be a major factor in promoting protein aggregation. At neutral pH the fusion peptide of FHA2 is thought to be exposed, enabling this construct to bind to membranes even prior to acidification [34]. It is these neutral structures that, upon acidification, either evolve into fusion intermediates or become inactivated. Upon protonation, the fusion peptide already in the membrane becomes more hydrophobic and promotes protein association. This does not necessarily mean that the fusion peptide itself aggregates in the membrane and in fact the lack of extensive spin–spin interaction between spin-labeled fusion peptides of FHA2 indicates that this region of the protein is monomeric [34]. There is evidence that another region of the protein, the kinked loop region of residues 108–115, may promote the low pH-induced aggregation of FHA2 [18]. With intact HA the fusion peptide is covered by the HA1 subunit and cannot enter the membrane at neutral pH [35]. HA binds to the target membrane through interaction of the HA1 subunit with receptor sites. No attempt was made to

image the HA protein as it is a water-insoluble integral membrane protein and would have to be incorporated into the bilayer by other methods. However, from the crystal structure one can appreciate that the fusion peptide in the neutral pH form, although buried within the protein structure, is only approx. 3 nm from the putative location of the transmembrane segment and hence the membrane into which the HA is inserted [2]. Hence upon acidification the fusion peptide can rapidly enter the membrane and promote protein association in the same manner that it does with FHA2. Insertion of the fusion peptide into the viral membrane was recently hypothesized to be of importance for the mechanism of fusion [36]. Of course there are differences between the intact HA and FHA2. It has been suggested that the energy derived from the extension of the coiled coil in HA can drive the formation of an energetically charged dimple in the membrane [36]. This cannot be the source of energy with FHA2 that is already in an extended conformation at neutral pH. In addition, FHA2 promotes only hemifusion, while HA facilitates full fusion. Nevertheless, there are a large number of similarities in the characteristics of the merger caused by these two proteins [11,12]. In this work we have shown that FHA2 tends to aggregate in membranes at low pH, as has already been shown with HA.

BHA has the same neutral pH conformation as the ectodomain of the intact HA. However, unlike HA, BHA is a water-soluble protein and has no hydrophobic attachment to the membrane. Like HA, BHA also binds to the membrane through interactions between the HA1 subunit and sialic acid residues. However, in this orientation the fusion peptide of BHA is on the opposite side of the protein (Fig. 6), approx. 8.5 nm from the membrane [2]. It is known that influenza virus will be inactivated at lower pH in the absence of target membrane [37]. Hence upon acidification the fusion peptide aggregates outside of the membrane and does not allow for protein aggregates to bind to the membrane surface but rather causes the formation of rosettes in solution or of aggregates bound to defect regions in the case of the supported bilayers. The present results would thus suggest that the juxtaposition of the influenza fusion peptide close to or within a membrane is an important prerequisite for the promotion of fusion by acidification.

Acknowledgements

This work was supported by the Canadian Institutes of Health Research.

References

[1] J. Brunner, C. Zugliani, R. Mischler, Biochemistry 30 (1991) 2432–2438.
[2] I.A. Wilson, J.J. Skehel, D.C. Wiley, Nature 289 (1981) 366–373.
[3] P.A. Bullough, F.M. Hughson, J.J. Skehel, D.C. Wiley, Nature 371 (1994) 37–43.
[4] W. Weissenhorn, A. Dessen, L.J. Calder, S.C. Harrison, J.J. Skehel, D.C. Wiley, Mol. Membr. Biol. 16 (1999) 3–9.
[5] S.A. Wharton, L.J. Calder, R.W. Ruigrok, J.J. Skehel, D.A. Steinhauer, D.C. Wiley, EMBO J. 14 (1995) 240–246.
[6] T. Shangguan, D.P. Siegel, J.D. Lear, P.H. Axelsen, D. Alford, J. Bentz, Biophys. J. 74 (1998) 54–62.
[7] C. Bottcher, K. Ludwig, A. Herrmann, M. van Heel, H. Stark, FEBS Lett. 463 (1999) 255–259.
[8] D.K. Takemoto, J.J. Skehel, D.C. Wiley, Virology 217 (1996) 452–458.
[9] R. Jiricek, G. Schwarz, T. Stegmann, Biochim. Biophys. Acta 1330 (1997) 17–28.
[10] C.H. Kim, J.C. Macosko, Y.G. Yu, Y.K. Shin, Biochemistry 35 (1996) 5359–5365.
[11] R.F. Epand, J.C. Macosko, C.J. Russell, Y.K. Shin, R.M. Epand, J. Mol. Biol. 286 (1999) 489–503.
[12] E. Leikina, D.L. LeDuc, J.C. Macosko, R.F. Epand, R.M. Epand, Y.K. Shin, L.V. Chernomordik, Biochemistry, in press.
[13] E. Jo, J. McLaurin, C.M. Yip, P. George-Hyslop, P.E. Fraser, J. Biol. Chem. 275 (2000) 34328–34334.
[14] J. McLaurin, D. Yang, C.M. Yip, P.E. Fraser, J. Struct. Biol. 130 (2000) 259–270.
[15] Y. Fang, S. Cheley, H. Bayley, J. Yang, Biochemistry 36 (1997) 9518–9522.
[16] J. Yang, L.K. Tamm, T.W. Tillack, Z. Shao, J. Mol. Biol. 229 (1993) 286–290.
[17] J. Mou, D.M. Czajkowsky, Z. Shao, Biochemistry 35 (1996) 3222–3226.
[18] C.H. Kim, J.C. Macosko, Y.K. Shin, Biochemistry 37 (1998) 137–144.
[19] R.W. Compans, H.D. Klenk, L.A. Caliguiri, P.W. Choppin, Virology 42 (1970) 880–889.
[20] D.J. Muller, D. Fotiadis, S. Scheuring, S.A. Muller, A. Engel, Biophys. J. 76 (1999) 1101–1111.

[21] C. Moller, M. Allen, V. Elings, A. Engel, D.J. Muller, Biophys. J. 77 (1999) 1150–1158.
[22] J.L. Hutter, J. Bechhoefer, J. Appl. Phys. 73 (1993) 4123–4129.
[23] J. Muthing, F. Unland, Glycoconjugate J. 11 (1994) 486–492.
[24] Y. Suzuki, T. Nakao, T. Ito, N. Watanabe, Y. Toda, G. Xu, T. Suzuki, T. Kobayashi, Y. Kimura, A. Yamada, Virology 189 (1992) 121–131.
[25] Y. Suzuki, Prog. Lipid Res. 33 (1994) 429–457.
[26] D.L. LeDuc, Y.K. Shin, R.F. Epand, R.M. Epand, Biochemistry 39 (2000) 2733–2739.
[27] R.C. Bethell, N.M. Gray, C.R. Penn, Biochem. Biophys. Res. Commun. 206 (1995) 355–361.
[28] T. Korte, A. Herrmann, Eur. Biophys. J. 23 (1994) 105–113.
[29] S.J. Morris, D.P. Sarkar, J.M. White, R. Blumenthal, J. Biol. Chem. 264 (1989) 3972–3978.
[30] R. Blumenthal, D.P. Sarkar, S. Durell, D.E. Howard, S.J. Morris, J. Cell Biol. 135 (1996) 63–71.
[31] T. Danieli, S.L. Pelletier, Y.I. Henis, J.M. White, J. Cell Biol. 133 (1996) 559–569.
[32] H. Ellens, J. Bentz, D. Mason, F. Zhang, J.M. White, Biochemistry 29 (1990) 9697–9707.
[33] O. Gutman, T. Danieli, J.M. White, Y.I. Henis, Biochemistry 32 (1993) 101–106.
[34] J.C. Macosko, C.H. Kim, Y.K. Shin, J. Mol. Biol. 267 (1997) 1139–1148.
[35] Y. Gaudin, R.W. Ruigrok, J. Brunner, J. Gen. Virol. 76 (1995) 1541–1556.
[36] M.M. Kozlov, L.V. Chernomordik, Biophys. J. 75 (1998) 1384–1396.
[37] A. Puri, F.P. Booy, R.W. Doms, J.M. White, R. Blumenthal, J. Virol. 64 (1990) 3824–3832.